

The Branched Polymer Growth Model Revisited

Ubiraci P. C. Neves ^{1,*}, André L. Botelho ¹, and Roberto N. Onody ²

¹*Departamento de Física e Matemática, Faculdade de Filosofia, Ciências e Letras de Ribeirão Preto
Universidade de São Paulo - Ribeirão Preto - SP, Brazil and*

²*Departamento de Física e Informática, Instituto de Física de São Carlos,
Universidade de São Paulo - São Carlos-SP, Brazil*

The branched polymer growth model (BPGM) has been employed to study the kinetic growth of ramified polymers in the presence of impurities. In this article, the BPGM is revisited on the square lattice and a subtle modification in its dynamics is proposed in order to *adapt* it to a scenario closer to reality and experimentation. This new version of the model is denominated the *adapted branched polymer growth model* (ABPGM). It is shown that the ABPGM preserves the functionalities of the monomers and so recovers the branching probability b as an input parameter which effectively controls the relative incidence of bifurcations. The critical locus separating infinite from finite growth regimes of the ABPGM is obtained in the (b, c) space (where c is the impurity concentration). Unlike the original model, the phase diagram of the ABPGM exhibits a peculiar reentrance.

Keywords: Branched Polymer, Critical Transition, Reentrant Phase

PACS numbers: 05.70.Jk; 64.60.-i; 64.60.Ht

I. INTRODUCTION

The statistical mechanics of polymers has become a very prolific research area. During the last decades, many models have been proposed to describe the configurational properties of linear and branched polymers and a variety of methods have been employed to study these systems. The classic model for a linear polymer in dilute solution (or at high temperature) is the self-avoiding walk (SAW) [1, 2]. On the other hand, connected clusters (lattice animals) provided a good model for branched polymers in the dilute limit [3].

The kinetic growth walk (KGW) was proposed as an alternative model to describe the irreversible growth of linear polymers [4-6]. Like the SAW, every KGW chain does not intercept itself. But whereas in a SAW the next step is randomly chosen from among *all* nearest-neighbor sites (excluding the previous one), in a KGW the choice is among the *unvisited* sites [4]. Therefore the KGW is less sensitive to attrition. Besides, although both models span the same set of configurations, the N -step SAW chains are *all* equally weighted while the statistical weights of the KGW chains can be different. Nevertheless, it was shown that both models present the same critical exponents [6].

Later, Lucena *et al.* [7] generalized the KGW in order to allow for branching as well as for impurities. This generalized model (which became known as the branched polymer growth model - BPGM) was found to exhibit an interesting phase transition (due to competition between hindrances and branching) separating infinite from finite growth regimes [7]. In the following years, several authors have studied the BPGM [8-15]. The topological

and dynamical aspects of the model were investigated [8]. Besides, the system was shown to achieve the criticality through a self-organization growth mechanism [12] and to exhibit a transition from rough to faceted boundaries for large values of the branching probability [8, 13]. The model was also studied through an exact enumeration of bond trees and ergodicity violation was discussed [14]. The question of the universality class of the BPGM was also investigated. In contrast to the common belief that branched polymers belong to the universality class of lattice animals [16, 17], the study of the growth process in chemical l -space with estimates of structural exponents led to the proposal that the BPGM belongs to the universality class of percolation [10, 11]. On the Bethe lattice, this proposal is based on analytical results [11]. A further analysis using finite-size scaling techniques led to the conclusion that the BPGM is *not* in the same universality class of percolation in two dimensions [15].

In the present paper, we revisit the BPGM on the square lattice. We point out that, although the input parameter b is named branching probability, it does not have effective control of the relative incidence of bifurcations (branches) in the simulated polymers. This seems to be an undesirable aspect of the model since the degree of branching is an important quantity that is usually measured in real ramified polymers. Besides, according to the growth rules of the BPGM, a monomer which is chosen to bifurcate (with probability b) but has only one empty nearest neighbor site is compelled to grow linearly thus changing its functionality from 3 to 2. In real experiments this change is not allowed since the concentrations of polymers with different functionalities are fixed. In order to preserve the functionalities of the monomers as well as to recover the meaning of the branching probability b , we propose a subtle modification in the dynamics of the BPGM. So this new version of the model aims to *adapt* it to a more realistic scenario and is called the

*Electronic address: ubiraci@ffclrp.usp.br

adapted branched polymer growth model (ABPGM). In the following sections, we define the ABPGM and present the phase diagram in the (b, c) space. This diagram is found to exhibit a peculiar reentrance. We introduce the concept of *frustration* and compare the *effective branching rate* b_{ef} with the input parameter b for both the original and adapted models. Our results concerning the ABPGM are shown to be much closer to the ideal behavior $b_{ef} = b$. Finally, we present a discussion based on the clusters topologies of both models.

II. THE ADAPTED BRANCHED POLYMER GROWTH MODEL

First of all, let us review the BPGM. Consider a $L \times L$ square lattice with a certain concentration c of sites randomly filled by impurities. At the initial time $t = 0$, the polymer starts growing from a monomer seed located at the center of the lattice towards a random empty nearest-neighbor site. At time $t = 1$, this chosen site is occupied by a monomer (growing tip) which now *may* bifurcate or follow in one direction (linear growth). The growth directions are randomly chosen among the available ones (those which lead to empty neighbors) in a clockwise way. At every time t ($t \geq 2$), the process is repeated for all actual monomeric ends following the sequence of their appearances. If a polymer end has *no* empty nearest-neighbor site then it is trapped in a “cul de sac” and stops growing (it is then called a *dead end*). If only one adjacent site is available then the linear growth is obligatory. If at least two adjacent sites are empty then the growing end bifurcates with probability b or follows linearly with probability $1 - b$. In a particular experiment of the BPGM, the polymer growth is simulated according to the above rules. Depending on the values of parameters b and c , the polymer can either grow indefinitely or stop growing (*die*) at a finite time if all its current tips are dead ends. The experiment is finished either when the polymer touches the frontier of the lattice (*infinite* polymer) or when it dies (*finite* polymer). The ensemble over which averages are performed is constituted by a great number N_e of experiments.

Each polymer configuration of the BPGM can be identified with a self-avoiding loopless graph (*bond tree*) although the reciprocal is not always true [8]. Thus the BPGM can be mapped into a particular *subset* of the ensemble of all possible bond trees. These tree graphs have been applied in models of branched polymers and can be classified by the number N of bonds and the number N_k of vertices with k bonds [18]. In a typical finite polymer configuration of the BPGM, one may find twofold and threefold sites representing monomers of functionalities 2 and 3, respectively. The monomer seed and dead ends represent monofunctional monomers. Tetrafunctional units are impossible in this model once trifurcations are not allowed. For a tree graph generated by the BPGM one has the following constraints [18]:

$$\sum_{k=1}^3 N_k = N + 1 \quad (1)$$

and

$$\sum_{k=1}^3 kN_k = 2N. \quad (2)$$

The occurrence of bifurcations in the model determines the relative incidence of trifunctional monomers (branches). This is basically the *degree of branching* of the polymer, an important quantity that is usually measured in real ramified polymers. However, although the parameter b is named *branching probability*, we shall see that it does *not* have effective control of the relative amount of branches (bifurcations) in the BPGM. Indeed, according to the rules of the BPGM, the parameter b is not the probability that any tip bifurcates but instead it is the conditional probability that a tip *with two or more empty nearest neighbors* bifurcates. Every tip with just one vacant nearest-neighbor site grows linearly with probability equal to one. From another viewpoint, it would also be desirable to consider that any monomer that is linking to the polymer has an effective probability b of being a trifunctional unit. Even if this were considered in the BPGM, a problem would become evident. Any growing end chosen (with probability b) as a trifunctional monomer would *not* be able to bifurcate if only one vacant site were available. In this case, the functionality of the monomer would not be respected since (according to the BPGM) the growing end would forcibly follow a linear growth like a bifunctional monomer.

In order to preserve the functionalities of the monomers we propose a modification in the dynamics of the BPGM. Besides to make the model a little more realistic, our proposal turns the branching probability b into an effective control parameter of the relative frequency of bifurcations. So it *adapts* the model to a scenario closer to reality and experimentation. We denominate it the *adapted branched polymer growth model* (ABPGM).

The ABPGM is defined just like the BPGM except for the following differences:

1. In the process of polymerization, let a *free end* (a growing tip with at least one empty nearest-neighbor site) be a trifunctional monomer with probability b or a bifunctional monomer with probability $1 - b$. If the free end is a trifunctional monomer but there is only one empty nearest neighbor site then it stops growing and becomes a dead end.
2. At every time unit, all current sites on the front of growth of the polymer are visited in a *random* sequence.

We remember that in the BPGM, a free end with *just one* empty nearest neighbor grows linear with probability one while in the ABPGM, since bifurcation is impossible, the free end stops and becomes a *frustrated* dead end. This frustration seems to be preferable and more realistic than forcing a trifunctional monomer to turn into bifunctional monomer as it occurs in the BPGM. So, in our proposal, the relative incidence of bifunctional and trifunctional monomers does not depend on the topology of the cluster anymore and is only controlled by the branching probability parameter. The second difference is also important: in the BPGM all tips are *sequentially* visited in a clockwise manner following the sequence of births whereas in the ABPGM they are visited in a *random* way. The sequential update of the growth front of the polymer (in the BPGM) simulates the formation of parallel chains in the infinite phase (for high b and low c) like in a crystallization process. This mechanism leads to a faceted-to-rough transition that has been already studied [8, 13]. Figure 1a shows a typical BPGM configuration with faceted boundary generated with parameters $b = 0.5$ and $c = 0$ (for $L = 51$); the parallel ordering of chains is caused by the clockwise update of the growing tips. If we simulate the BPGM using the same set of parameters but with a random update instead of the clockwise update we get Figure 1b. In this case, two subsequent growing tips are probably located far apart so that they cannot produce parallel chains. The boundary is less faceted than before. Recently it has been shown that any deterministic growth order is *non-ergodic* in the sense that it spans only a subset of the space of all possible configurations [14]. Moreover, for the present purposes, this clockwise update mechanism is undesirable since the development of parallel chains corresponds to an increasing incidence of bifunctional monomers due mainly to geometrical effects rather than to the probability $1 - b$ itself. The relative incidence of bifurcations (which will be defined as *the effective branching rate* b_{ef} in section 4) is much smaller than input parameter b . Indeed, we anticipate that $b_{ef} \approx 0.15$ for the cluster of Figure 1a whereas $b_{ef} \approx 0.30$ for the one of Figure 1b; so the last rate (corresponding to a BPGM cluster generated with random update) is closer to the input value $b = 0.50$. The effective branching rate gets still closer to the input value if we simulate the ABPGM. Figure 1c is a typical ABPGM configuration (generated with those same parameters $b = 0.5$ and $c = 0$) and presents $b_{ef} \approx 0.43$; the faceted front of growth seems to disappear and vacancies can be found inside the cluster.

The main feature of the BPGM is the phase transition separating finite from infinite growth regime. Lucena *et al.* [7] have defined a critical branching probability b_c where the mean size of finite polymers diverges as $L \rightarrow \infty$. The critical value depends on the impurity concentration c and separates the finite phase ($b < b_c(c)$) from the infinite one ($b > b_c(c)$). The probability that a polymer grows indefinitely is null for small values of b and increases abruptly in the region of $b \approx b_c(c)$. This

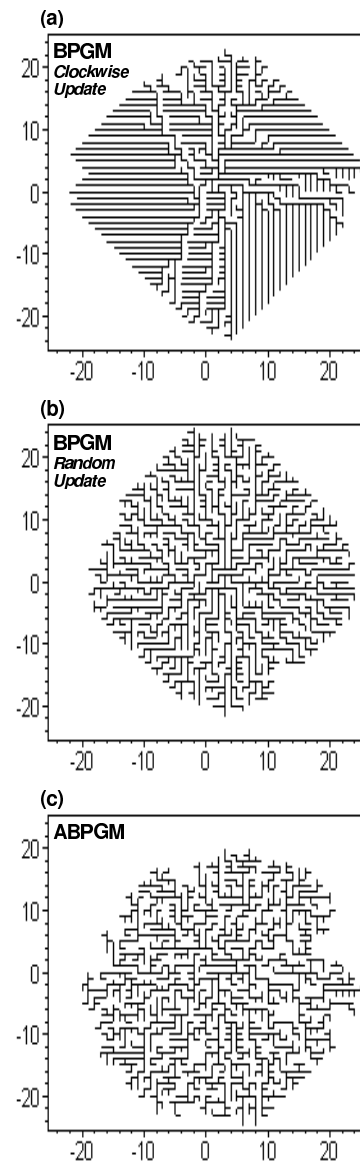


FIG. 1: Typical configurations simulated on a square lattice of size $L = 51$ with parameters $b = 0.5$ and $c = 0$ according to the BPGM rules with clockwise update of growing tips (a), BPGM with random update (b) and ABPGM (c). The corresponding effective branching rates are $b_{ef} \approx 0.15$, $b_{ef} \approx 0.30$ and $b_{ef} \approx 0.43$, respectively.

probability was estimated through the *fraction* P_∞ of infinite polymers in the ensemble of configurations of the BPGM [7]. In Figure 2a, we reproduce typical plots of P_∞ versus b at different values of c (with $N_e = 10^2$ experiments and $L = 1501$) for the BPGM. In Figure 2b, we present plots of P_∞ versus b at some values of c corresponding to simulations of the ABPGM with $N_e = 10^4$ experiments and $L = 1501$. For $c = 0$, the behavior of $P_\infty(b)$ is analogous to that of the BPGM but now the threshold is little bit higher ($b \approx 0.06$ for the ABPGM while $b \approx 0.055$ for the BPGM). This difference increases

with c . The most interesting characteristic of the present model may be observed when $c = 0.18$. For this value, the curve raises at $b \approx 0.32$, then presents a plateau (where $P_\infty(b) \approx 0.7$) and finally falls! By a finite-size scaling analysis we have verified that the height of the plateau does not change significantly in the limit $L \rightarrow \infty$. For $c = 0.19$, the behavior of $P_\infty(b)$ is gaussian shaped. This means that, for certain impurity concentrations, as b increases the system goes from a finite to an infinite phase and then becomes finite again! Indeed, this reentrance is confirmed in the next section when we determine the phase diagram of the ABPGM through an analysis of the correlation length.

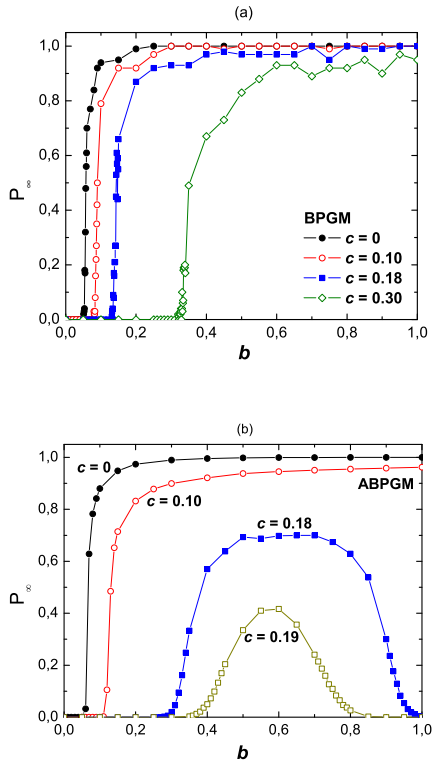


FIG. 2: Plots of the fraction of infinite polymers P_∞ versus b for the BPGM (a) and ABPGM (b).

III. THE PHASE DIAGRAM

The mean size of finite polymers is a measure of the *correlation length* ξ of the system. If a finite polymer is generated during a simulation, the sizes l_x and l_y of the smallest rectangle containing the cluster can be determined. The correlation length can then be calculated as $\xi = \langle (l_x l_y)^{1/2} \rangle$ where the average is performed over all experiments with finite polymers [7]. We show typical plots of ξ versus b corresponding to simulations of the BPGM (in Figure 3a) and ABPGM (in Figure 3b)

for different values of c and size $L = 1501$ (with 10^2 and 10^4 experiments respectively). Each plot of ξ versus b exhibits only one maximum except for plots of the ABPGM with $c > 0.175$ where two peaks are detected! It can be verified that all peaks of ξ do diverge when $L \rightarrow \infty$.

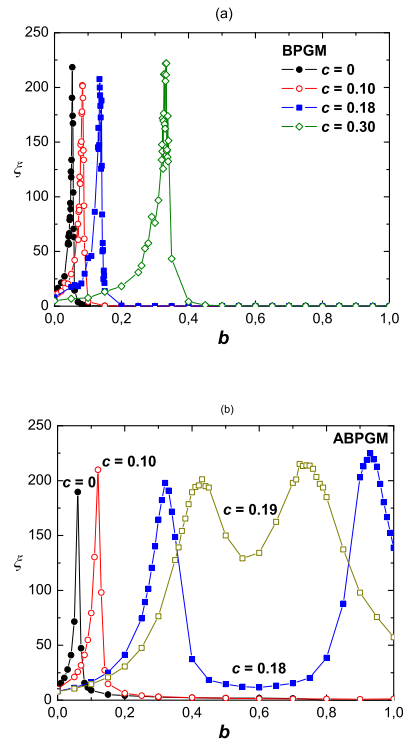


FIG. 3: Plots of the correlation length ξ of finite polymers versus the branching probability b for several impurity concentrations c in the cases: (a) BPGM and (b) ABPGM.

Let us first explain the behavior of ξ for the BPGM. For a fixed value of c and as b increases, the polymer is more likely to escape from steric hindrances and impurities so that the mean size grows to its highest value at some $b = b_0(L)$. Above this point, the system is defined to be in the infinite growth regime (of course, the true critical point is obtained in the thermodynamic limit $b_c = \lim_{L \rightarrow \infty} b_0(L)$). As b continues to increase, the fraction of infinite polymers grows and the finite polymers get smaller so that ξ decreases. As higher impurity concentrations hinder the growth, b_0 increases with c . The critical line of the BPGM is the locus (b_c, c) on which ξ diverges [7] and is shown in Figure 4 (dashed line).

Regarding the ABPGM, the same reasoning can explain the maximum of ξ (or the first maximum when there are two peaks). But now this peak is located on a higher branching probability $b_1 > b_0$ that compensates the occurrence of frustrated dead ends. Just above b_1 the system enters the infinite growth regime where it remains unless a second peak appears (at $b = b_2 > b_1$ for $c > 0.175$). In the latter case the system returns to the fi-

nite phase! This reentrance from infinite to finite growth regime is a peculiar feature of the ABPGM. For this modified model, there is a certain range of values of c where it is very probable that all free ends become frustrated (and stop growing) for a sufficiently large b so that the polymer growth is finite again. The ABPGM phase diagram is also shown in the Figure 4. The reentrant phase only exists for c in the small interval $[0.175, 0.195]$.

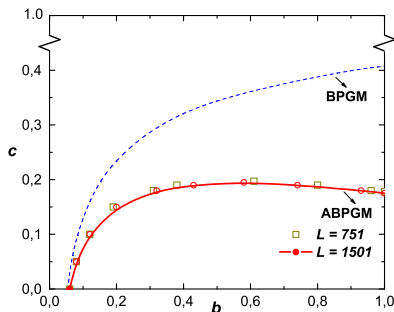


FIG. 4: The phase diagram of the models BPGM (dashed line) and ABPGM (solid line). Each critical line separates the infinite phase (at low values of c) from the finite one (at higher values of c).

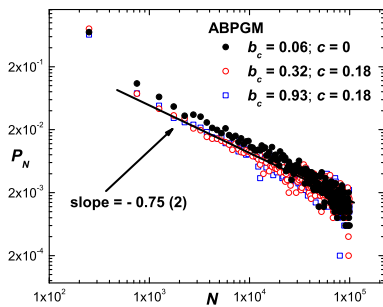


FIG. 5: Log-log plot of the distribution $P(N)$ of finite polymers with N bonds for simulations of the ABPGM (with $N_e = 10^4$ and $L = 1501$) at some points (b, c) on the critical line.

We have also measured the fraction $P(N)$ of finite polymers with N bonds. In Figure 5, we have a log-log plot of the polydispersion distribution $P(N)$ of the ABPGM on the critical line (running 10^4 experiments in a $L = 1501$ lattice). The three sets of data correspond to the critical points: $b_1 \approx 0.06$ and $c = 0$ (black dots); $b_1 \approx 0.32$ and $c = 0.18$ (open circles); $b_2 \approx 0.93$ and $c = 0.18$ (squares). The data are fitted by a straight line with slope -0.75 . So, on the critical line, $P(N)$ decays with N as a power law. We have verified that outside the

critical line, $P(N)$ decays exponentially with N . Lucena *et al.* [7] have found a similar behavior in the BPGM.

IV. THE FRUSTRATION AND THE EFFECTIVE BRANCHING RATE

The *frustration* is a desirable event which distinguishes the ABPGM from the original model. It is defined as the *interruption* of the growth of any free end which was chosen (with probability b) as a trifunctional monomer but is unable to bifurcate since only one nearest neighbor site is available. It prevents such a free end to continue its growth linearly like a bifunctional monomer (as occurs in the BPGM) and consequently controls the relative incidence of branches.

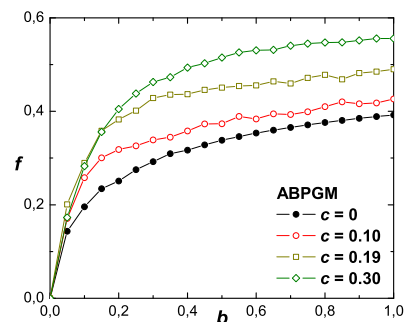


FIG. 6: The *frustration rate* f versus b for increasing values of c in the ABPGM ($L = 1501$ and $N_e \sim 10^3$).

Clearly, each polymer configuration of the ABPGM is also a bond tree which can be classified by the numbers N (of bonds) and N_k (of k -functional units). Besides, every *dead end* is a site which ceased to grow and so represents a monofunctional vertex; it can be subclassified as either a *trapped site* (if it is in a "cul de sac") or a *frustrated dead end* (otherwise). We denote by \tilde{N}_1 the number of frustrated dead ends. For the BPGM, $\tilde{N}_1 = 0$ since any free end never stops. In order to measure the relative incidence of frustrated ends among those free sites *chosen* as trifunctional monomers, we define the *frustration rate* as

$$f = \left\langle \frac{\tilde{N}_1}{\tilde{N}_1 + N_3} \right\rangle \quad (3)$$

where the average is performed over *all* experiments. For infinite polymers, the current sites on the front of growth should not be considered in the computation since their functionalities are undetermined.

According to the prior definition, $f = 0$ for any values of b and c in the BPGM. We remark that the null frustration of the BPGM does *not* mean that all free sites *chosen*

to bifurcate succeed but only that when they fail they are transformed in monomers with functionality two.

For the ABPGM, the frustration rate increases with b and c as it is shown in Figure 6. Indeed, both the excluded volume due to self-avoidance (which increases with b) and the impurities diminish the chance of success of any free end, so f is a monotonically increasing function of b and c .

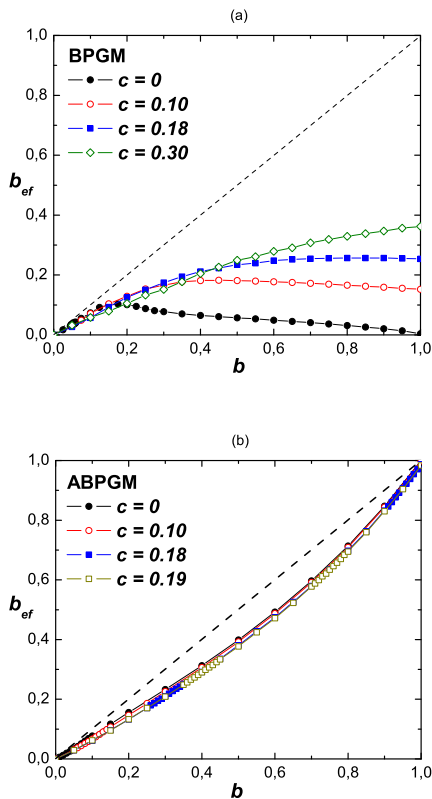


FIG. 7: The behavior of the *effective branching rate* b_{ef} versus the input parameter b for simulations of the BPGM (a) and ABPGM (b) on a large $L = 1501$ square lattice (with 10^2 and 10^4 experiments respectively). The dashed lines represent the ideal behavior $b_{ef} = b$.

The effectiveness of the input parameter b is evaluated by comparing it with the relative frequency of branches in a polymer configuration. For this purpose, we define the *effective branching rate* b_{ef} as the ratio between N_3 and $N_2 + N_3$ averaged over all experiments:

$$b_{ef} = \left\langle \frac{N_3}{N_2 + N_3} \right\rangle \quad (4)$$

The plots of b_{ef} versus b at different values of c for simulations of the BPGM and ABPGM (on a large $L = 1501$ square lattice) are shown in Figures 7a and 7b, respectively. The ideal behavior $b_{ef} = b$ is indicated as the dashed lines. Regarding the BPGM, there is evidently

a large discrepancy between the input parameter b and the output rate b_{ef} . For $c = 0$, b_{ef} increases with b up to a maximum (at $b \approx 0.2$) and then decreases to zero as $b \rightarrow 1$. This behavior is explained as follows: for small b , self-avoidance is reduced so that most sites trying to bifurcate succeed; but as b increases, parallel linear chains (like those of Figure 1a) are forcibly generated due to both the increasing excluded volume and the clockwise update. For higher values of c , the presence of impurities hampers the formation of linear chains and thus b_{ef} decreases slower (as a *concave* function). Anyway, for the BPGM, the discrepancy between b and b_{ef} gets more pronounced as $b \rightarrow 1$. On the contrary, for the ABPGM, b_{ef} always increases with b as a *convex* function (for any value of c) and the difference $b - b_{ef}$ is very small. In fact, for any c , the ratio b_{ef}/b is approximately equal to 1 for small b , decreases until about 0.8 for intermediate b and then returns to 1 as $b \rightarrow 1$. Such results corroborate the assertion that the input parameter b controls the relative incidence of branches in the adapted model.

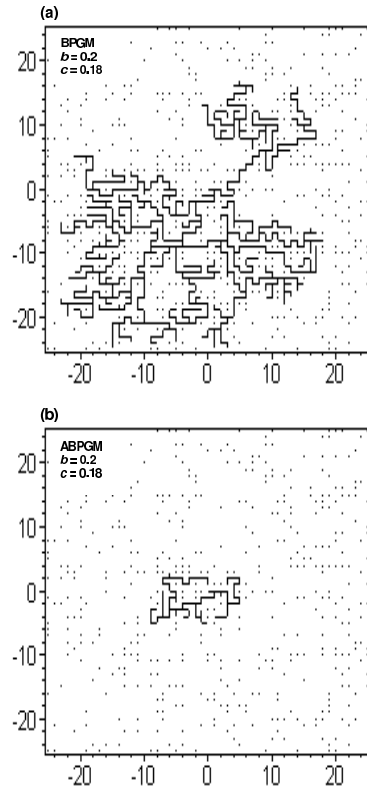


FIG. 8: Typical graphs of both the BPGM (a) and ABPGM (b) for $b = 0.2$ and fixed $c = 0.18$.

V. CONCLUSIONS

The *branched polymer growth model* (BPGM) was originally proposed [7] as a generalization of the *kinetic*

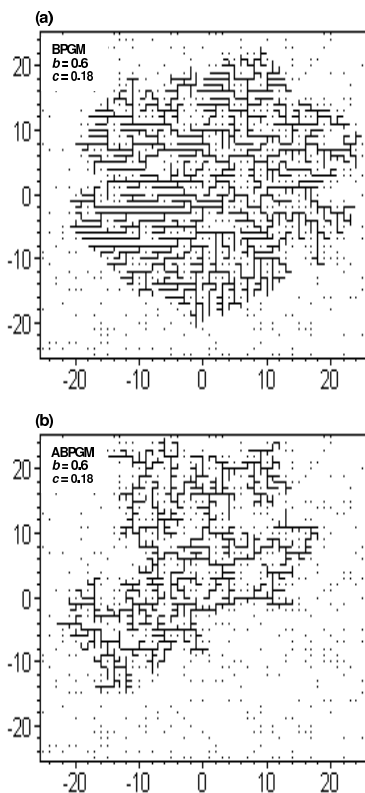


FIG. 9: Typical graphs of both the BPGM (a) and ABPGM (b) for $b = 0.2$ and fixed $c = 0.18$.

growth walk [4] in order to include the possibility of ramification of the polymer as well as the presence of impurities in the medium. The model was found to exhibit a finite-infinite transition due to competition between branching and hindrances.

In this paper, we have proposed an alteration in the dynamics of the BPGM so as to *adapt* the model to an experimental realism. We have called it the *adapted branched polymer growth model* (ABPGM). The main difference between our proposal and the original model regards to the growth mechanism of a monomer which is chosen to bifurcate (with probability b) but has just one empty nearest neighbor site. In the BPGM, such a monomer is transformed into a bifunctional unit so that it grows linearly (with probability one). In our adapted model, that monomer stops and becomes a frustrated dead end. This frustration reveals as preferable and more realistic than changing the monomer functionality from 3 to 2 (as it occurs in the BPGM). This subtle change in the algorithm together with a *random* update of the growing ends lead to the formation of polymers with new topological patterns and adjusted degrees of branching. Indeed, we have shown that the effective branching rate

b_{ef} is very much closer from the input parameter b in the ABPGM than in the original model.

We have found that the ABPGM presents a finite-infinite transition in the (b, c) space with a peculiar reen-

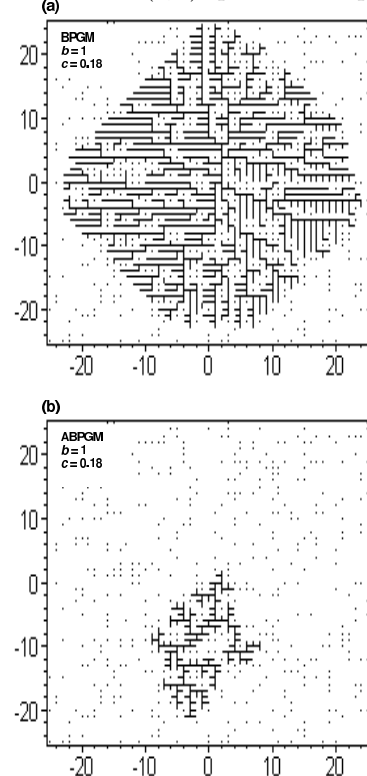


FIG. 10: Typical graphs of both the BPGM (a) and ABPGM (b) for $b = 1$ and fixed $c = 0.18$.

trant phase in the small interval $0.175 \leq c \leq 0.195$. At this instance, we compare some typical graphs of both the BPGM and ABPGM at the *fixed* impurity concentration $c = 0.18$ for three increasing values of b : 0.2, 0.6 and 1 (Figures 8, 9 and 10, respectively). For the BPGM, all the three corresponding configurations are *infinite* clusters whose boundaries change from rough to faceted as b increases. On the other hand, the typical ABPGM graph for $b = 0.2$ is a *finite* cluster (due to the occurrence of *both* trapped sites and frustrated dead ends); if $b = 0.6$ the cluster is *infinite* (since here higher branching overcomes dead ends) and if $b = 1$ the cluster is *finite* again (due to a high frustration rate).

We hope that the ideas presented here can add a new degree of physical understanding to the model as well as they can approximate it to the real ramified polymers.

This work has been supported by Brazilian Agencies CAPES, CNPq and FAPESP (through grant No. 96/05387-3).

[1] P. J. Flory, *Principles of Polymer Chemistry* (Cornell Univ. Press, Ithaca, NY, 1953).

[2] P.G. de Gennes, *Scaling Concepts in Polymer Physics*

- (Cornell Univ. Press, Ithaca, NY, 1979).
- [3] T. C. Lubensky and J. Isaacson, *Phys. Rev. A* **20**, 2130 (1979).
 - [4] I. Majid, N. Jan, A. Coniglio and H. E. Stanley, *Phys. Rev. Lett.* **52**, 1257 (1984).
 - [5] H. J. Herrmann, *Kinetics of Aggregation and Gelation* edited by F. Family and D. P. Landau (North-Holland, Amsterdam, 1984).
 - [6] J. W. Lyklema and K. Kremer, *J. Phys. A* **19**, 279 (1986).
 - [7] L. S. Lucena, J. M. Araújo, D. M. Tavares, L. R. da Silva and C. Tsallis, *Phys. Rev. Lett.* **72**, 230 (1994).
 - [8] U. P. C. Neves and R. N. Onody, *Physica A* **218**, 1 (1995).
 - [9] R. N. Onody and U. P. C. Neves, *J. Phys. A* **29**, L527 (1996).
 - [10] A. Bunde, S. Havlin and M. Porto, *Phys. Rev. Lett.* **74**, 2714 (1995).
 - [11] M. Porto, A. Shehter, A. Bunde and S. Havlin, *Phys. Rev. E* **54**, 1742 (1996).
 - [12] J. S. Andrade Jr., L. S. Lucena, A. M. Alencar and J. E. Freitas, *Physica A* **238**, 163 (1997).
 - [13] L. S. Lucena, L. R. da Silva and Stéphane Roux, *Physica A* **266**, 86 (1999).
 - [14] R. N. Onody, C. A. P. Silva, *Physica A* **284**, 23 (2000).
 - [15] S. S. Botelho and F. D. A. Aarão Reis, *Phys. Rev. E* **63**, 011108-1 (2000).
 - [16] T. C. Lubensky and J. Isaacson, *Phys. Rev. Lett.* **41**, 829 (1978).
 - [17] S. Havlin, Z. V. Djordjevic, I. Majid and H. E. Stanley, *Phys. Rev. Lett.* **53**, 178 (1984).
 - [18] C. J. Camacho and M. E. Fisher, J. P. Straley, *Phys. Rev. A* **46**, 6300 (1992). Data sets available in AIP document No. PAPS PRLAA-466300-49, ref. 9212C-1307.